

## CLINICAL INVESTIGATION

# Compression of the middle cerebellar tract by posterior fossa tumors before and after Gamma Knife radiosurgery studied with diffusion tensor imaging

Herwin Speckter<sup>1,2</sup>, Jose Bido<sup>1</sup>, Giancarlo Hernandez<sup>1</sup>, Diones Rivera<sup>1</sup>, Luis Suazo<sup>1</sup>, Santiago Valenzuela<sup>1</sup>, Cesar Gonzalez<sup>2</sup> and Peter Stoeter<sup>1,2</sup>

<sup>1</sup>Centro Gamma Knife Dominicano, CEDIMAT, Plaza de la Salud, Santo Domingo, Dominican Republic

<sup>2</sup>Department of Radiology, CEDIMAT, Plaza de la Salud, Santo Domingo, Dominican Republic

*Correspondence to: Herwin Speckter; Department of Radiology and Centro Gamma Knife Dominicano, CEDIMAT, Plaza de la Salud, Santo Domingo, Dominican Republic; E-mail: [hspeckter@cedimat.net](mailto:hspeckter@cedimat.net); Phone: +1 809 565 9989; Fax: +1 809 565 7925*

*(Received: June 25, 2018; Accepted: September 18, 2018)*

### ABSTRACT

**Purpose:** To investigate if clinically asymptomatic compression of the middle cerebellar tract by extracerebral posterior fossa tumors can produce changes in diffusion tensor imaging (DTI) parameters and if these changes return to normal after Gamma Knife radiosurgery (GKRS).

**Material and methods:** In 22 patients (12 female, mean age 53.8 years) with posterior fossa tumors (14 schwannomas and 8 meningiomas), the middle cerebellar tract was tracked using DTI data. DTI parameters, such as fractional anisotropy (FA), mean diffusivity (MD), axial diffusivity (AD) and radial diffusivity (RD) within these tracts were determined separately on the tumor side and on the contra-lateral side. As a surrogate parameter of tract compression, we used the distance between a tangential line extending between the anterior, not affected part of the pons and the cerebellum, and the furthest extension of the tumor into the lateral rim of the pons. In a subgroup of 15 patients, DTI parameters were recorded after a follow-up of more than 2 years (mean follow-up time 37.5 months) after GKRS and compared to initial findings.

**Results:** Before GKRS, all DTI parameters within the compressed tract had increased. The increase in MD correlated significantly with the degree of tract compression ( $c = 0.443$ ,  $p < 0.05$ ). Follow-up examinations after GKRS showed reduction in FA and AD, whereas MD and RD increased. After correction for time elapsed after treatment and tumor type, the changes of MD and AD following treatment correlated significantly with the reduction of tract compression, but not with radiation dose.

**Conclusion:** Although without obvious clinical symptoms, disorders of the middle cerebellar tract, as in the case of posterior fossa tumors, persist after reduction of tumor size. Because of the significant correlation between the change of parameters and the reduction of tract compression, initial compression and consequent relief are regarded as the main factors responsible for persistent disorders of the middle cerebellar tract. Radiosurgery dose did not contribute significantly to changes in DTI parameters.

**Keywords:** middle cerebellar tract; Gamma Knife radiosurgery; diffusion tensor imaging

## INTRODUCTION

Severe compression or displacement of the white matter tract induced by tumors or other space-occupying lesions of the brain can remain asymptomatic on clinical examination, unless the tracts are disrupted or infiltrated by tumor tissue. During the last decade, diffusion tensor imaging (DTI) has proved its value in the detection of micro-structural white matter changes of these tracts in a standardized way.<sup>17</sup> In order of increasing loss of fiber integrity and orientation, and consequent changes in DTI parameters, four different patterns of tract alteration induced by cerebral neoplasm can be distinguished: displacement, edematous changes, infiltration and destruction.<sup>7</sup> DTI-based tractography has been used increasingly to guide neurosurgery and predict outcome in tumors and vascular malformations.<sup>2,16,15</sup>

Since 2005,<sup>13</sup> tractography based on DTI data has been integrated into Gamma Knife radiosurgery (GKRS) and has enabled significant reductions in radiation dose applied to the newly defined “organ at risk”, the cortico-spinal tract.<sup>8</sup> However, quantitative longitudinal studies using the tractography technique have not been carried out in GKRS, except in the treatment of trigeminal neuralgia cases, where significant changes in fractional anisotropy (FA), radial diffusivity (RD) and axial diffusivity (AD) have been reported after high dose GKRS.<sup>6</sup>

This longitudinal study aims to compare DTI parameters derived from reconstructed tracts: (i) to measure the influence of simple tract compression on the absence of edematous or infiltrative alterations on DTI parameters before GKRS; and (ii) to follow these changes over time after GKRS.

## MATERIAL AND METHODS

This project was approved by the Institutional Review Board of our center and informed consent was given by all participants.

### *Patients, Neoplasms and Follow-up*

Retrospectively, we included 22 patients (12 females and 10 males) with a mean age of 53.8 (8.7–79.0) years presenting with 14 schwannomas and 8 meningiomas of the posterior fossa with various degrees of indentation of the ventral outline of the pons (Table 1). All participants had not been operated on before and had been previously subjected to magnetic resonance

imaging (MRI) including DTI before GKRS. None of the 22 patients presented peri-tumoral edema on T2w imaging, neither before GKRS, nor on follow-up MRIs. The meningiomas were slightly larger than the schwannomas (mean volume: 9.9 vs. 8.0 ml), whereas the indentation of the pons, which we used as a surrogate parameter for tract compression, was nearly the same (9.2 vs. 9.0 mm). From this group, we report DTI parameter differences between the middle cerebellar tract on the tumor and contralateral side.

In a subgroup of 15 patients, follow-up MRIs were available more than 2 years after treatment (mean time 37.5 months, range 24.4 to 61.6 months). From this subgroup, we report DTI parameter changes in the middle cerebellar tract after GKRS and their correlation with changes in tumor volume and indentation of the middle cerebellar tract.

### *Gamma Knife Radiosurgery*

GKRS was performed on a Leksell Gamma Knife unit (Model 4C, Elekta/Sweden). The margin dose applied to schwannomas varied from 12 to 13 Gy while that applied to meningiomas ranged from 12 to 15 Gy, with the exception of one schwannoma case treated by hypo-fractionated GKRS (3 × 5 Gy, corresponding to a single fraction equivalent dose of 9.4 Gy, applying an alpha/beta ratio of 2.4 Gy, according to Vernimmen<sup>22</sup>). The treatment was planned on a Leksell GammaPlan workstation (Version 10.1, Elekta/Sweden) by adjusting the margin dose to fit the outer border of the lesion and to avoid undesired dose to vital organs at risk (cochlea, cranial nerves, brain stem), keeping the coverage index as high as possible (mean: 97.0 %). The 10 Gy dose volume covered the ipsilateral half of the pons at least partially in all cases, whereas the contralateral side was not included.

### *Magnetic Resonance Imaging*

MRI was performed on a 3 T scanner (Achieva, Philips/Netherlands). Routine T2-, FLAIR- and T1-weighted sequences before and after injection of contrast medium were acquired, as well as the following DTI sequence: 32 gradient directions, b = 0 and 800 s/mm<sup>2</sup>, measured voxel size 2 × 2 × 2 mm, 60 slices covering the whole head, SENSE factor 2, scanning time 4.5 min.

### *Postprocessing*

DTI data was postprocessed of by the software package ExploreDTI ([www.providi-lab.org](http://www.providi-lab.org)),<sup>9</sup> including co-registration of T1-weighted images, tractography of

**Table 1.** Patients and neoplasms before GKRS

Tumor	No. of cases	Volume (ml)	Indentation of middle cerebellar tracts (mm)
Schwannomas	14	8.0 ± 5.2	12.0 ± 5.0
Meningiomas	8	9.9 ± 7.1	9.7 ± 5.2

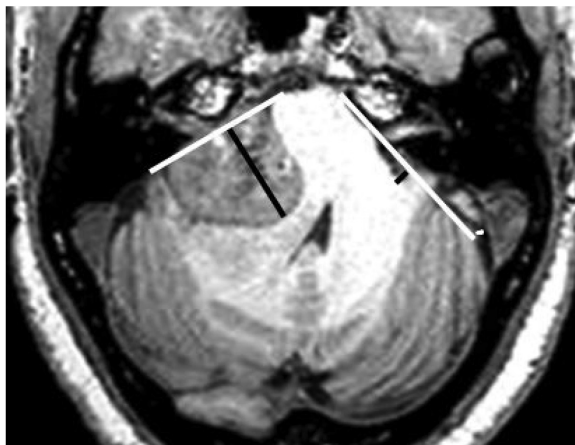


**Figure 1.** Calculation of impression of outline of pons  
On both sides, tangential lines were drawn between the non-deformed anterior part of the pons and the posterior part of the cerebellum (white lines) as well as vertical lines to the maximum of indentation on the tumor side with respect to the pons outline in an identical position on the contra-lateral side (black lines). The difference between the two vertical lines was taken as a surrogate parameter for indentation.

both the whole brain and middle cerebellar tract from a sagittal seeding ROI placed in the center of the base of the pons and a tracking algorithm, which limited the seed and tracking FA threshold to 0.2. The split functions allowed the division of the common fiber bundle originating from the seed ROI into an ipsi- and a contra-lateral part, and the measurement of DTI parameters, such as FA, AD, RD and mean diffusivity (MD) independently on both sides. To correct for systematic measurement deviations in the MRI system over time, we used the difference between DTI parameters on the tumor side and the contra-lateral side for follow-up evaluation.

Tumor volumes and indentation of the outer contour of the pons were measured on the GammaPlan workstation from contrast enhanced T1-weighted images. To determine the degree of pons indentation by the tumor, we drew a tangential line from the outline ventral to the indentation, to the lateral outline of the cerebellum dorsal to the indentation and measured the vertical dis-

tance of this line to the maximum of the indentation. On the contralateral side, we measured the vertical difference between an identically placed tangential line and the mark where the cerebellum arises from the pons. The extent of indentation of the pons was defined as the difference between the two vertical distances, measured on the same image (Figure 1).

Differences in DTI parameters between ipsi- and contra-lateral tracts before and after GKRS were demonstrated to be significant by the paired t-test. Using the functionality of the statistical package SPSS 15.0 (SPSS, Inc., Chicago, IL, USA), we performed a partial correlation analysis between radiation dose, DTI parameters, pons indentation and their change over time as core variables, while correcting for such control variables as tumor type, patient age (before GKRS) and time to follow-up (after GKRS). Correction for tumor type was performed to adjust for possible differences in tumor environment, while correction for patient age takes into account DTI parameter changes due to aging. The level of significance was set at  $p \leq 0.05$ . Finally, we conducted a stepwise multiple linear regression analysis with changes in difference of DTI parameters as dependent variables and changes in pons indentation, radiation dose, type of lesion and time elapsed from GKRS as independent variables.

## RESULTS

### Before GKRS

Depending of the tumor size, compression of the ipsi-lateral middle cerebellar tract (Figure 1, Table 1) ranged from rather low (indentation of the pontine outline of 4.1 mm) to severe (indentation of 20.6 mm). There was a significant correlation between tumor size and extent of indentation (correlation coefficient: 0.574,  $p < 0.01$ ).

Compared to the contralateral side, all DTI parameters of the middle cerebellar tract on the tumor side increased (Table 2), and this rise reached significance in the case of FA (0.517 vs. 0.496,  $p < 0.05$ ) and AD ( $1.359 \times 10^{-3} \text{ mm}^2/\text{s}$  vs.  $1.287 \times 10^{-3} \text{ mm}^2/\text{s}$ ,  $p < 0.01$ ). Apart from FA, where correlation was very low (corrected for tumor type and patient age), diffusion parameters correlated positively, with the degree of tract compression being significant in the case of MD (correlation coefficient 0.443,  $p < 0.05$ ).

### Follow-up after GKRS

Control rate achieved for the meningioma cases was 100%, with an average volumetric tumor reduction of

**Table 2.** DTI Parameters of the middle cerebellar tract before GKRS (22 patients)

Middle cerebellar tract	FA	MD ( $10^{-3} \times \text{mm}^2/\text{s}$ )	AD ( $10^{-3} \times \text{mm}^2/\text{s}$ )	RD ( $10^{-3} \times \text{mm}^2/\text{s}$ )
Tumor side	0.517 ± 0.039	0.836 ± 0.076	1.359 ± 0.113	0.576 ± 0.071
Contra-lateral side	0.496 ± 0.033	0.807 ± 0.060	1.287 ± 0.074	0.564 ± 0.064
Difference between sides	0.021 ± 0.036*	0.029 ± 0.070	0.072 ± 0.097**	0.012 ± 0.066
Correlation of side difference with tract indentation <sup>a</sup>	-0.065	0.443, p = 0.05	0.407	0.360

<sup>a</sup>After correction for tumor type and patient age.

t-test tumor side vs. contralateral side: \*p < 0.05, \*\*p < 0.01

0.6 % per month, range -0.18–1.32 %, after GKRS. Control rate achieved for the schwannoma cases was 92.8%, with an average volumetric tumor reduction of 1.5 % per month, range -3.02–4.55 %, after GKRS.

The subgroup of 15 patients who underwent follow-up examinations more than 2 years after GKRS, again showed increased DTI parameter values (with the exception of FA) on the tumor side compared to the contralateral side (Figure 2, Table 3). The increases in MD ( $0.831 \times 10^{-3} \text{ mm}^2/\text{s}$  vs.  $0.801 \times 10^{-3} \text{ mm}^2/\text{s}$ ) and of AD ( $1.315 \times 10^{-3} \text{ mm}^2/\text{s}$  vs.  $1.213 \times 10^{-3} \text{ mm}^2/\text{s}$ ) reached significance (p < 0.05).

Although differences before and after GKRS were rather small on the non-affected side (FA: 0.001, MD:  $0.002 \times 10^{-3} \text{ mm}^2/\text{s}$ , AD:  $0.010 \times 10^{-3} \text{ mm}^2/\text{s}$ , RD:  $0.002 \times 10^{-3} \text{ mm}^2/\text{s}$ ), we used these side differences rather than the values measured on each side to assess changes in parameters after GKRS in order to correct for deviations of scanner performance during an extended time interval of more than 2 years. These changes over time (side differences before GKRS minus side differences after GKRS) were positive in FA and AD, which means a reduction in previously increased parameters on the tumor side ( $0.023$  and  $0.028 \times 10^{-3} \text{ mm}^2/\text{s}$ ), and negative in MD and RD, which means an additional increase on the tumor side ( $-0.004 \times 10^{-3} \text{ mm}^2/\text{s}$  and  $-0.019 \times 10^{-3} \text{ mm}^2/\text{s}$ ).

The changes in differences of DTI parameters between sides correlated positively with the reduction of indentation of the middle cerebellar tract in all cases (after correction for tumor type and time elapsed after GKRS) and reached significance for MD (correlation coefficient: 0.671, p = 0.002) and AD (correlation coefficient: 0.684, p = 0.010). Positive correlation means that in all parameters a larger reduction in a specific parameter after GKRS goes together with a larger reduction in tract compression. As for radiation dose, correlation of this change in side differences of DTI parameters over time was lower for all parameters and without significance.

The multiple linear regression analysis showed that indentation of cerebellar tract accounted for around 50% of the variance in change of DTI parameter differences (R<sup>2</sup> for MD: 0.557, R<sup>2</sup> for AD: 0.511 and R<sup>2</sup> for RD: 0.522), whereas none of the other variables, such as radiation dose, type of lesion and time elapsed after GKRS, added significant explanatory power to the regression model.

## DISCUSSION

To the best of our knowledge, no studies had been published at the time of drafting this report on the effect of posterior fossa tumor compression on DTI parameters of the middle cerebellar tract. The fiber tracking technique has demonstrated its reliability by substantial inter-rater agreement when confined to a single center and a specific tracking methodology.<sup>3</sup> In contrast to previous studies,<sup>14,4,24,5</sup> we decided to include only patients with extra-axial tumors in order to avoid tract invasion or disruption, and to examine the middle cerebellar tract to minimize the influence of the position of the ROI on measurement results. Due to their transverse course in the base of the pons, these tracts can be tracked and followed to both sides from a single, centrally placed ROI, which allows the bundle to be split into an ipsi- and a contra-lateral part and DTI parameters to be measured independently on both sides. In this way, the parameters of the non-affected contra-lateral tract allow correction for scanner-related changes in DTI measurements over time.

Before GKRS, we saw a pattern that is slightly different from the “pattern 1” described previously in merely displaced tracts,<sup>7</sup> where the value of FA is maintained or slightly reduced. Our more severely compressed middle cerebellar tracts showed increases in all four DTI parameters that were significant in the case of FA and AD, whereas MD correlated significantly with the degree of tract compression. The latter find-



**Table 3.** Difference of DTI parameters before and after GKRS (subgroup of 15 patients)

Middle cerebellar tract	FA	MD ( $10^{-3} \times \text{mm}^2/\text{s}$ )	AD ( $10^{-3} \times \text{mm}^2/\text{s}$ )	RD ( $10^{-3} \times \text{mm}^2/\text{s}$ )
Tumor side before GKRS	0.516 ± 0.045	0.845 ± 0.069	1.372 ± 0.106	0.582 ± 0.070
Contra-lateral side before GKRS	0.492 ± 0.034	0.817 ± 0.061	1.299 ± 0.077	0.576 ± 0.062
Difference tumor side vs. contra-lateral side before GKRS	0.024 ± 0.037*	0.029 ± 0.058	0.073 ± 0.093**	0.006 ± 0.056
Tumor side after GKRS	0.493 ± 0.036	0.849 ± 0.107	1.344 ± 0.146	0.602 ± 0.095
Contra-lateral side after GKRS	0.491 ± 0.037	0.815 ± 0.070	1.289 ± 0.080	0.578 ± 0.071
Difference tumor side vs. contra-lateral side after GKRS	0.002 ± 0.040	0.034 ± 0.059*	0.055 ± 0.093*	0.024 ± 0.060
Change in side difference before minus post GKRS	0.022 ± 0.041	-0.005 ± 0.054	0.018 ± 0.088	-0.018 ± 0.056
Correlation of change in side difference before/after GKRS with improvement in indentation <sup>a</sup>	0.208	0.671, p = 0.002	0.684, p = 0.010	0.355
Correlation of change in side difference before/after GKRS with margin dose to the tumor <sup>a</sup>	0.196	0.297	0.427	0.038

<sup>a</sup>After correction for tumor type and time elapsed after GKRS.  
t-test tumor side vs. contralateral side: \*p < 0.05, \*\*p < 0.01

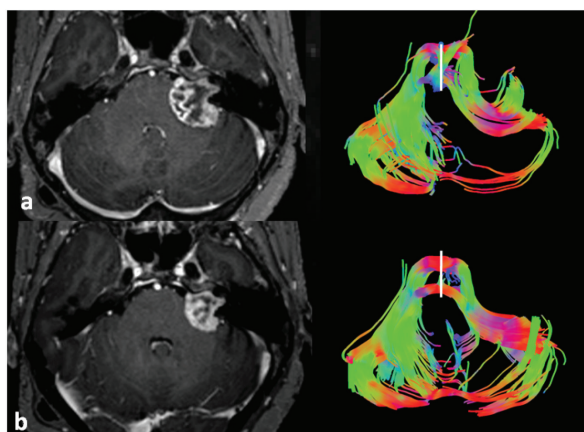


**Figure 2.** 57 year old female. Schwannoma and the middle cerebellar tract before and after GKRS. **a:** Before GKRS, a contrast-enhanced image of a large schwannoma (left) and large deviation and compression of the middle cerebellar tract (right). **b:** 4½ years after GKRS with a margin dose of 12 Gy, a substantial reduction in tumor volume as well as tract deviation and compression were shown. The seeding ROI, from where tracking is initiated to track a common fiber bundle, is marked by a white line (right images). Middle cerebellar tract parameters are then calculated separately on both sides from the common fiber bundle split by this line.

ing can be seen as an unspecific indication of edema or necrosis. In some cases, it is possible that hypoperfusion of the ipsilateral cerebellar hemisphere was also involved.<sup>25,26</sup> The rather low and insignificant increase in RD could be due to some, however limited, degree of myelin damage.<sup>23</sup> The increase in FA might be due to the dense packing of tracts, and both effects, the packing and limited degree of fiber damage, may account for the significant increase in AD.<sup>19,1</sup> Severe axonal damage can be excluded, because in that case we would expect a reduction in AD due to debris from disrupted membrane barriers.<sup>21</sup>

After GKRS, patients showed a reduction in FA and AD, which correlated positively with a reduction in tract compression, confirming our hypothesis that the increases in both parameters on the tumor side before GKRS were mainly due to compression. The mean of MD did not change very much after GKRS and the mean of RD even showed an increase. However, the changes in MD correlated significantly with the reduction of tract compression, possibly due to a general increase in diffusion in a now decompressed fiber bundle.

In the case of RD, an additional factor, namely axonal injury after a long-standing and just partially relieved compression or after radiation, requires consideration. Such an injury could have caused the per-

sistent increase and further rise during follow-up of this parameter. In all cases, the middle cerebellar tract on the tumor side had been exposed in some areas to at least 10 Gy. This dosage is indeed capable of inducing changes in DTI parameter values of peritumoral white matter,<sup>18</sup> whereas the radiation tolerance of the pyramidal tract has been reported to be much higher. Although the latter tract carries a 5% risk of motor complications at a dose maximum of 23 Gy,<sup>11</sup> others like the optic radiation or the arcuate fibers, are less resistant.<sup>12,10</sup> Significant changes in DTI parameters have been observed after GKRS in the perilesional brain tissue isodose volume irradiated with doses in the range 5–15 Gy.<sup>20</sup>

In our cases, however, the correlation between RD increase and tract compression reduction, although not significant, was much higher than that between RD increase and radiation dose (0.355 vs. 0.038). The results of the linear regression analysis, where reduction of tract compression, but not radiation dose, was able to account for over 50% of the variation in DTI parameter changes, point to the same conclusion: that compression or decompression after tumor volume reduction are the main factors responsible for DTI parameter changes under these circumstances, and not the radiation dose applied.

## CONCLUSION

In line with previous reports of increases in FA and AD in compressed, but not infiltrated, tracts, this study shows that after decompression due to successful GKRS, compression-related FA and AD alterations are reduced, whereas increases in MD and RD persist or even rise. Whether the latter effect is due to minor but ongoing axonal damage caused by compression or just a detection of pre-existing alterations hidden in the initial scan, where compression was more severe, cannot be determined. Our results demonstrate that long-standing compression induces damage to the long white matter tract and underline the importance of tumor size reduction by GKRS. The contribution of radiation dose to this damage, however, appears to be insignificant.

## ACKNOWLEDGMENTS

### *Authors' disclosure of potential conflicts of interest*

The authors have nothing to disclose.

### *Author contributions*

Conception and design: Herwin Speckter, Peter Stoeter

Data collection: Herwin Speckter, Jose Bido, Giancarlo Hernandez, Diones Rivera, Luis Suazo, Santiago Valenzuela, Cesar Gonzalez, Peter Stoeter

Data analysis and interpretation: Herwin Speckter, Jose Bido, Giancarlo Hernandez, Diones Rivera, Luis Suazo, Santiago Valenzuela, Cesar Gonzalez, Peter Stoeter

Manuscript writing: Herwin Speckter, Peter Stoeter

Final approval of manuscript: Herwin Speckter, Jose Bido, Giancarlo Hernandez, Diones Rivera, Luis Suazo, Santiago Valenzuela, Cesar Gonzalez, Peter Stoeter

## ABBREVIATIONS

- GKRS: Gamma Knife Radiosurgery
- DTI: Diffusion Tensor Imaging
- FA: Fractional Anisotropy
- MD: Mean Diffusivity
- AD: Axial Diffusivity
- RD: Radial Diffusivity

## REFERENCES

1. Alexander AL, Hurley SA, Samsonov AA, Adluru N, Hosseinbor AP, Mossahebi P, et al. Characterization of cerebral white matter properties using quantitative magnetic resonance imaging stains. *Brain Connect*. 2011;1:423-46.
2. Bagadia A, Purandare H, Misra BK, Gupta S. Application of magnetic resonance tractography in the perioperative planning of patients with eloquent region intra-axial brain lesions. *J Clin Neurosci*. 2011;18:633-9.
3. Christidi F, Karavasilis E, Samiotis K, Bisdas S, Papanikolaou N. Fiber tracking: A qualitative and quantitative comparison between four different software tools on the reconstruction of major white matter tracts. *Eur J Radiol Open*. 2016;3:153-61.
4. Faraji AH, Abhinav K, Jarbo K, Yeh FC, Shin SS, Pathak S, et al. Longitudinal evaluation of corticospinal tract in patients with resected brainstem cavernous malformations using high-definition fiber tractography and diffusion connectometry analysis: preliminary experience. *J Neurosurg*. 2015;123:1133-44.
5. Gavin CG, Ian Sabin H. Stereotactic diffusion tensor imaging tractography for Gamma Knife radiosurgery. *J Neurosurg*. 2016;125:139-146.
6. Hodaie M, Chen DQ, Quan J, Laperriere N. Tractography delineates microstructural changes in the trigeminal nerve after focal radiosurgery for trigeminal neuralgia. *PLoS One*. 2012 Mar;7(3):e32745.
7. Jellison BJ, Field AS, Medow J, Lazar M, Salamat MS, Alexander AL. Diffusion tensor imaging of cerebral white matter: a pictorial review of physics, fiber tract anatomy, and tumor imaging patterns. *AJNR Am J Neuroradiol*. 2004;25:356-69.

8. Kawasaki K, Matsumoto M, Kase M, Nagano O, Aoyagi K, Kageyama T. Quantification of the radiation dose to the pyramidal tract using tractography in treatment planning for stereotactic radiosurgery. *RadiolPhys Technol.* 2017;10:507-514.
9. Leemans A, Jeurissen B, Sijbers J. ExploreDTI. Version 4.8.6. PROVIDI Lab. [cited 2016 June 23]; Available from: <http://www.providi-lab.org>.
10. Maruyama K, Koga T, Kamada K, Ota T, Itoh D, Ino K, et al. Arcuate fasciculus tractography integrated into Gamma Knife surgery. *J Neurosurg.* 2009;111:520-6.
11. Maruyama K, Kamada K, Ota T, Koga T, Itoh D, Ino K, et al. Tolerance of pyramidal tract to gamma knife radiosurgery based on diffusion-tensor tractography. *Int J Radiat Oncol Biol Phys.* 2008;70:1330-5.
12. Maruyama K, Kamada K, Shin M, Itoh D, Masutani Y, Ino K, et al. Optic radiation tractography integrated into simulated treatment planning for Gamma Knifesurgery. *J Neurosurg.* 2007;107:721-6.
13. Maruyama K, Kamada K, Shin M, Itoh D, Aoki S, Masutani Y, et al. Integration of three-dimensional corticospinaltractography into treatment planning for gamma knife surgery. *J Neurosurg.* 2005;102:673-7.
14. Miller P, Coope D, Thompson G, Jackson A, Herholz K. Quantitative evaluation of white matter tract DTI parameter changes in gliomas using nonlinear registration. *Neuroimage.* 2012;60:2309-15.
15. Nimsy C, Bauer M, Carl B. Merits and Limits of Tractography Techniques for the Uninitiated. *Adv Tech Stand Neurosurg.* 2016;43:37-60.
16. Potgieser AR, Wagemakers M, van Hulzen AL, de Jong BM, Hoving EW, Groen RJ. The role of diffusion tensor imaging in brain tumor surgery: a review of the literature. *ClinNeurolNeurosurg.* 2014;124:51-8.
17. Pujol S, Wells W, Pierpaoli C, Brun C, Gee J, Cheng G, et al. The DTI Challenge: Toward Standardized Evaluation of Diffusion Tensor Imaging Tractography for Neurosurgery. *J Neuroimaging.* 2015;25:875-82.
18. Ravn S, Holmberg M, Sørensen P, Frøkjær JB, Carl J. Differences in supratentorial white matter diffusion after radiotherapy – new biomarker of normal brain tissue damage? *Acta Oncol.* 2013;52:1314-9.
19. Schonberg T, Pianka P, Hendler T, Pasternak O, Assaf Y. Characterization of displaced white matter by brain tumors using combined DTI and fMRI. *Neuroimage.* 2006;30:1100-11.
20. Speckter H, Bido J, Hernandez G, Rivera D, Suazo L, Valenzuela S, et al. Perilesional changes in diffusion tensor imaging parameters after Gamma Knife stereotactic radiosurgery. *Innovative Neurosurg.* 2015;3:35-42.
21. Sun SW, Liang HF, Le TQ, Armstrong RC, Cross AH, Song SK. Differential sensitivity of in vivo and ex vivo diffusion tensor imaging to evolving optic nerve injury in mice with retinal ischemia. *Neuroimage.* 2006; 32:1195–1204.
22. Vernimmen FJ, Slabbert JP. Assessment of the alpha/beta ratios for arteriovenous malformations, meningiomas, acoustic neuromas, and the optic chiasma. *Int J Radiat Biol.* 2010;86:486-98.
23. Wu YC, Field AS, Duncan ID, Samsonov AA, Kondo Y, Tudorascu D, et al. High b-value and diffusion tensor imaging in a canine model of dysmyelination and brain maturation. *Neuroimage.* 2011;58:829–837.
24. Yao Y, Ulrich NH, Guggenberger R, Alzarhani YA, Bertalanffy H, Kollias SS. Quantification of Corticospinal Tracts with Diffusion Tensor Imaging in Brainstem Surgery: Prognostic Value in 14 Consecutive Cases at 3T Magnetic Resonance Imaging. *World Neurosurg.* 2015;83:1006-14.
25. Tamamoto F, Kuwashima K, Shiraishi A, Kyogoku S, Shirakata A, Sumi Y, Katayama H. Influence of cerebellopontine angle tumor on cerebellar circulation--possibility of remote effect to the cerebellum. *Kaku Igaku* 1993;30:273-281.
26. Cohen BA, Knopp EA, Rusinek A, Liu S, Gonen O. Brain compression without global neuronal loss in meningiomas: whole-brain proton MR spectroscopy report of two cases. *AJNR Am J Neuroradiol* 2005;26:2178-2182